Studies on the Shapes of Si^{28}, S^{32}, and Ar^{36} via Deuteron Scattering*

M. C. MERMAZ,† C. A. WHITTEN, JR.,‡ AND D. A. BROMLEY
A. W. Wright Nuclear Structure Laboratory, Yale University, New Haven, Connecticut 06520

(Received 13 June 1969)

Deuteron elastic and inelastic scattering on $_{14}Si_{14}^{28}$, $_{16}S_{16}^{32}$, and $_{18}Ar_{18}^{36}$ was studied with an 18-MeV deuteron beam from the Yale MP tandem Van de Graaff accelerator. Optical-model and distorted-wave Born-approximation analyses of the experimental angular distributions were performed. The deformation parameters $|\beta_2|$ and $|\beta_3|$, extracted in this manner, are in accord with the corresponding parameters extracted from electromagnetic deexcitation lifetimes in those cases where the electromagnetic lifetimes of the states involved in the inelastic scattering have been measured. The experimental angular distributions were also analyzed through a coupled-channel approach. This method of analysis permitted extraction of more complete spectroscopic information concerning the nuclei under study, namely, the even-even $N=Z$ nuclei in the second half of the $2s$-$1d$ shell. The conclusions drawn regarding Si^{28} from the present work are not definite; however, the indications are that Si^{28} has an oblate static deformation, with excited states comprising a $K=0$ rotational band based on the ground state. The strong octupole vibration (the 6.88-MeV 3^- level) in Si^{28} is to some degree in contradiction with this conclusion. In the case of S^{32}, the results of the coupled-channel calculations indicate that the levels of S^{32} up to an excitation energy of 5 MeV are well explained on the assumption that S^{32} is an almost spherical vibrational nucleus. The results for Ar^{36} are quite similar to those for S^{32}; however, the data are unfortunately less clear, since a number of the most important levels appear in the experimental spectrum as unresolved doublets. Spherical shell-model calculations have been found to be in excellent accord with the spectroscopic factors measured in this laboratory for deuteron-induced stripping and pickup reactions on these nuclei. These data, together with extensive spectroscopic measurements here and elsewhere on lighter-mass nuclei in the s-d shell, suggest that in moving into the shell from O^{16} a pronounced static prolate deformation develops rapidly, reaching its maximum in the vicinity of $A=21$–23; subsequently, this deformation is reduced, and in the vicinity of $A=28$ it reverses sign to yield a weak, poorly stabilized oblate shape, which by $A=32$ has returned to a spherical equilibrium configuration which is retained to the end of the shell. These experimental findings are not reproduced by the simplest Hartree-Fock calculations, which predict a more pronounced oblate deformation in the upper half of the shell.

1. INTRODUCTION

IT has long been recognized[1–4] that the s-d shell contained regions of pronounced collectivity and, presumably, correspondingly pronounced static deformations of the nuclear equilibrium shapes. The question of the detailed behavior of this deformation with mass number throughout the shell has remained open since the initial discovery of collectivity in this mass region[1] and is an important one in establishing the depth of contemporary understanding of nuclear structure in this region.

It has been suggested[5] that (d, p), (d, t) and (d, d') experiments, particularly on even-even nuclei in the shell, could provide relevant information concerning this behavior of the equilibrium nuclear shapes with increasing nucleon number. The (d, p) and (d, t) reactions provide important probes for the particle and hole structure relative to the even-even cores; the (d, d') results hold promise of distinguishing between excitation spectra of vibrational character based on a spherical equilibrium shape and of rotational character based on a statically deformed shape, particularly when subjected to coupled-channel analyses.

Recognizing the relative paucity of such data in the upper half of the s-d shell, we have concentrated on the three target nuclei Si^{28}, S^{32}, and Ar^{36}, and have carried out the three types of measurements noted above at incident deuteron energies of 18 MeV for the (d, d') and (d, p) measurements and at 21 MeV for the (d, t) measurements. We report herein on the deuteron scattering measurements and analyses; in subsequent papers we shall consider the stripping and pickup results and their analyses, respectively.

Two types of theoretical analysis were applied to the experimental scattering data: (1), a distorted-wave Born approximation (DWBA) analysis using the code JULIE; (2) a coupled-channel analysis using the code JUPITOR-1. The DWBA analysis, in principle, permits determination of spin assignments for various excited levels through comparison of theoretical predictions with the experimentally determined angular distributions; and, in the case of one-step excitation processes,

* Work supported in part by the U. S. Atomic Energy Commission under Contract No. AT(30-1)3223.
† NATO Fellow on leave of absence from the Center for Nuclear Research, Saclay, France.
‡ Present address: Department of Physics, University of California, Low Angeles, Calif.
[1] A. E. Litherland, E. B. Paul, G. A. Bartholomew, and H. E. Gove Phys. Rev. **102**, 208 (1956).
[2] D. A. Bromley, H. E. Gove, and A. E. Litherland, Can. J. Phys. **35**, 157 (1957).
[3] A. E. Litherland, H. McManus, E. B. Paul, D. A. Bromley, and H. E. Gove, Can. J. Phys. **36**, 1057 (1957).
[4] H. E. Gove, in the *Proceedings of the International Conference on Nuclear Structure, Kingston, Canada, 1960*, edited by D. A. Bromley and E. W. Vogt (The University of Toronto Press, Toronto Canada 1960).
[5] G. Ripka, in the *Proceedings of the International Conference on Nuclear Physics, Gatlinburg, Tenn. 1967*, edited by R. L. Becker (Academic Press, Inc., New York, 1967), p. 833.

the absolute magnitude of the deformation parameter β—but not its sign—may also be determined. However, the DWBA method of analysis does not distinguish between vibrational and rotational modes of excitation, nor is this method well suited for studying levels whose excitation proceeds via a two-step process, e.g., two-phonon levels. On the other hand, the coupled-channel analysis can, in principle, describe quite completely the excitation of levels via two-step processes. This latter analysis can also, in some cases, distinguish between vibrational and rotational modes of excitation.

In brief, while the present measurements suggest that Si^{28} has a relatively weak static oblate deformation, they also indicate that this deformation rapidly dissolves, so that S^{32}, Ar^{36}, and presumably all nuclei in the upper part of the *s-d* shell are characterized by an essentially spherical equilibrium shape. This is in marked contrast to the situation in the $A=21$–23 region, where recent studies, in this laboratory and elsewhere, have established the existence of effective rigid body moments of inertia and suggest that these nuclei may indeed be the best rotor nuclei in the entire periodic table.[6] While this latter behavior is reproduced by the Hartree-Fock calculations[7] for this shell, that found in the upper end of the shell is not, in that the calculations predict a larger region of more pronounced oblate deformation than is found experimentally.

A review of the available information relevant to the equilibrium shapes throughout the *s-d* shell is in preparation and will be published in the near future.[8]

2. EXPERIMENTAL PROCEDURE

The experiments reported herein were performed in a 30-in. Ortec scattering chamber using an 18.00-MeV deuteron beam from the Yale MP tandem Van de Graaff accelerator. A two-counter telescope of solid-state detectors, standard linear electronics, and a Landis-Goulding type of particle identifier, constructed in this laboratory, were used to identify and energy-analyze the charged-particle reaction products. The particle spectra were stored in a 4096-channel Nuclear Data multichannel analyzer. The target conditions were continuously monitored by a further solid-state detector placed at a laboratory angle of 65°; this angle corresponded to a relative maximum in the 18-MeV elastic deuteron cross section for the nuclei involved in these experiments, and thus minimized statistical counting uncertainties.

In the $Si^{28}(d, d')$ experiment, a self-supported foil, $\sim$200 $\mu g/cm^2$ thick, of natural silicon (Si^{28} 92.7% abundant) which was a mixture of the chemical forms SiO and SiO_2 was used. In the $S^{32}(d, d')$ and $Ar^{36}(d, d')$ experiments, a gas cell target was used having a cell wall of 0.1-mil-thick Havar foil.[9] The gas cell was maintained at approximately 20-cm Hg pressure in these experiments. The sulfur target was H_2S gas (S^{32} 95.0% abundant) purchased from a commercial source, while the Ar^{36} gas was separated by the Yale Isotope Separation Group and was made available for these experiments by Dr. A. Howard and Dr. W. W. Watson, to whom we are much indebted.

3. ABSOLUTE CROSS-SECTION DETERMINATIONS

In the case of the $Si^{28}(d, d')$ experiment, the absolute cross sections were determined by measuring α-particle elastic scattering on silicon at 4.00 MeV, and deuteron elastic scattering on silicon at 18.00 MeV under the same experimental conditions of target condition and position and of detector geometry. The α-particle elastic-scattering angular distributions on silicon were found to obey the Rutherford scattering law for all angles below at least 90°. Consequently, for the same number of incident particles, the ratio of the α-particle and deuteron counting rates at a given angle was equal to the ratio of the α-particle 4.00-MeV Rutherford cross section and the deuteron 18.00-MeV elastic cross section in the laboratory system. In the case of deuteron inelastic scattering cross sections on silicon, due account was taken of the fact that the silicon target was only 92.27% Si^{28}. This comparison method for determining absolute cross sections was particularly appealing in the case of our silicon target, whose exact composition in terms of SiO and SiO_2 was unknown. We estimate conservatively that the absolute cross sections for deuteron elastic and inelastic scattering on Si^{28} are determined to considerably better than 10%.

In the case of the gas cell experiments using H_2S and Ar^{36} gas, two main difficulties were encountered in the determination of accurate, absolute deuteron scattering cross sections. Local heating of the gas along the beam path changed the effective gas density as a function of the beam current; the beam currents used in these experiments varied from about 10 nA at the most forward angles to about 500 nA at back angles. In the case of the sulfur experiments, the H_2S gas was cracked by the beam—mainly, we believe, at the entrance and exit foils—so that the amount of H_2S gas in the cell decreased as a function of time. In the case of the $Ar^{36}(d, d')$ experiments, we were able to estimate the heating effects quite accurately by plotting the ratio of monitor counts to integrated charge as a function of beam current and extrapolating this plot to zero beam

[6] R. Lindgren, R. Hirko, J. Pronko. A. J. Howard, and D. A. Bromley Bull. Am. Phys. Soc. **13**, 1371 (1968).
[7] J. Bar-Touv and I. Kelson Phys. Rev. **142**, 599 (1966).
[8] D. A. Bromley, M. C. Mermaz, C. A. Whitten, A. J. Howard, and J. Pronko (to be published).
[9] Purchased from the Hamilton Watch Company, Lancaster, Pa.

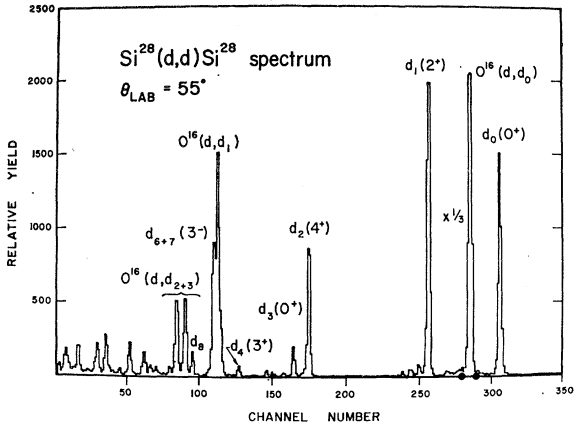

FIG. 1. Deuteron spectrum from Si^{28} obtained with a solid-state detector telescope at a deuteron incident energy of 18 MeV.

current or no heating effect. In the case of the $S^{32}(d, d')$ experiments, the cracking of the H_2S introduced additional errors, but the gas cell pressure was measured before and after each angular run, so that the average pressure during each run was known accurately. Furthermore, in the $S^{32}(d, d')$ experiments, there was a slight air contamination present in the gas cell. Taking all these effects into account, we estimate that the $S^{32}(d, d')$ and $Ar^{36}(d, d')$ absolute cross sections were determined to well within 15% and 10%, respectively. However, since the gas cell was continuously monitored by the monitor detector, the relative cross sections are established to a much higher degree of accuracy (statistically limited) than the absolute cross sections.

4. EXPERIMENTAL RESULTS WITH OPTICAL MODEL AND DWBA ANALYSES

A. Qualitative Results

Angular distributions were measured for $Si^{28}(d, d')$ scattering from 15° to 120°, for $S^{32}(d, d')$ scattering from 15° to 135°, and for $Ar^{36}(d, d')$ scattering from 15° to 150° in the laboratory. Figure 1 presents the deuteron spectrum obtained at 55° for the $Si^{28}(d, d')$ reaction. Figure 2 presents the deuteron spectrum obtained at 60° for the $S^{32}(d, d')$ reaction, while Fig. 3 presents the deuteron spectrum obtained at 60° for the $Ar^{36}(d, d')$ reaction. In all three spectra it should be noted that the first 2^+ level and the first 3^- level are strongly excited. Except where noted we shall take the excitation energies from the compilation of Endt and Van der Leun.[10]

The most direct interpretation of the Si^{28} spectrum is that the $K=0$ rotational band having members 0^+, 2^+, and 4^+ is being excited; this follows both from the strong excitation of these three states as compared to any others, and from the fact that these excitations are in reasonable accord with a $J(J+1)$ rotor spectrum prediction. On the other hand, the first excited 0^+ in Si^{28} at 4.98 MeV (d_3) is weakly excited, as is the 3^+ level at 6.28 MeV (d_4). This latter 3^+ level most probably has a $(1d_{5/2}^{-1}\, 2s_{1/2})$ particle-hole configuration, and is known to have a very weak electromagnetic transition matrix element to the ground state (Ref. d of Table II); it is thus not part of the collective excitation spectrum of Si^{28}.

No evidence was found at any angle for population of the second excited 0^+ state in Si^{28}, at 6.68 MeV, known as yet only from the $O^{16}(O^{16}, \alpha)Si^{28}$ studies carried out at Chalk River.[11] This may reflect the supposition, based on the abnormally long lifetime of this state against electromagnetic deexcitation to the first 2^+ state, that it may be the first state of opposite deformation sign to the ground state, i.e., a prolate state in an oblate equilibrium nucleus.

It is of interest to note that recent measurements[12] on the $Mg^{24}(Li^7, t)Si^{28}$ reaction have shown relatively weak population of members of the ground-state rotational band in Si^{28} but very strong population of the 0^+ state at 6.68 MeV. Inasmuch as Mg^{24} is definitely prolate in shape, it might be argued that simple α-particle transfer would populate preferentially prolate states in Si^{28}. This data might, therefore, support the argument that this state was the lowest prolate state in Si^{28}. A similar situation holds in the case of Si^{29}, which we also believe to be oblate in its ground-state configuration. On the reasonable assumption that Al^{27} is also prolate in its ground state, the failure of the $Al^{27}(He^3, p)Si^{29}$ reaction[13] to populate the low levels of Si^{29} strongly and the strong population of a state $\sim$4.5 MeV in excitation again suggests that the latter may be the lowest prolate state.

The 3^- octupole level at 6.88 MeV is indeed the only

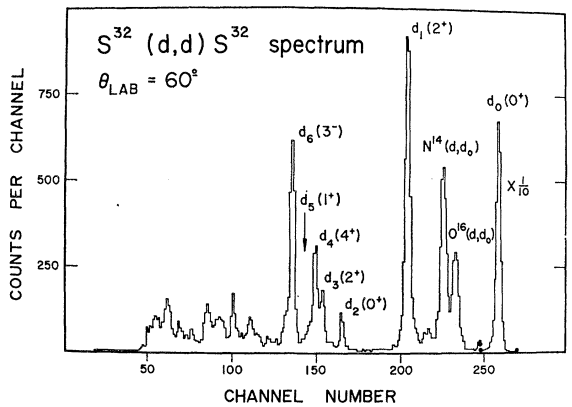

FIG. 2. Deuteron spectrum from S^{32} obtained with a solid-state detector telescope at a deuteron incident energy of 18 MeV.

[10] P. M. Endt and C. Van der Leun, Nucl. Phys. A105, 1 (1967).

[11] R. W. Ollerhead, Bull. Am. Phys. Soc. 13, 87 (1968).

[12] K. Wittner, B. Rosner, and K. Bethge (private communication).

[13] L. Meyer-Schutzmeister *et al.* (private communication).

other level in the Si^{28} excitation spectrum which is significantly populated in the inelastic deuteron scattering, and, as will be noted later, the strength of this excitation can be interpreted as favoring a predominantly vibrational, rather than rotational, structure for Si^{28}.

In striking contrast to the spectrum of Fig. 1, that of Fig. 2 for scattering on S^{32} shows structure to be expected for a spherical vibrator nucleus. The 0^+, 2^+, 4^+ triplet of levels (d_2, d_3, and d_4) occurs at roughly twice the excitation energy of the first 2^+ excitation, as would be expected for a two-phonon excitation of the ground state. Whereas the 2^+ state is at an excitation of 2.237 MeV, the triplet levels are at 3.78, 4.29, and 4.47 MeV, respectively. As in the case of Si^{28}, the only other strongly excited state is the 3^- octupole state at 5.01 MeV; in particular, the 1^+ level at 4.70 MeV is very weakly excited, if at all, consistent with its description as a $(1d_{3/2}^{-1}, 2s_{1/2})$ particle-hole configuration.

The Ar^{36} spectrum of Fig. 3 is significantly more complex and less amenable to a simple collective interpretation. The one-phonon 2^+ state at 1.97 MeV is very strongly excited, and a possible two-phonon triplet having assignments 0^+, 2^+ and 4^+ at excitations of 4.33, 4.44, and 4.41 MeV, respectively, is discernible although the 0^+ (d_3) excitation is especially weak at this particular observation angle. The dominant excitation, apart from the first 2^+ state, is clearly the 3^- octupole state at 4.178 MeV.

There appears to be significant population in this case of at least three more known negative parity states in Ar^{36}, namely, the 3^-, 5^-, and 4^- states at excitations of 4.96, 5.17 and 5.89 MeV, respectively; we shall examine below the hypothesis that these states may be members of a quadrupole-octupole two-phonon multiplet. No other higher states are involved to any substantial degree in the deuteron inelastic scattering.

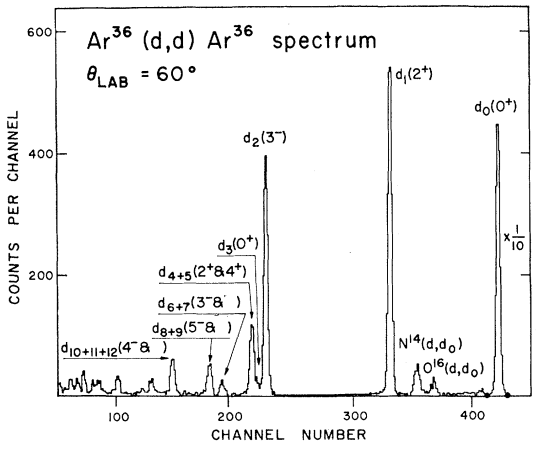

FIG. 3. Deuteron spectrum from Ar^{36} obtained with a solid-state detector telescope, at a deuteron incident energy of 18 MeV. In the case of the deuteron groups to the higher excited multiplets, the data suggest that the dominant excitation involves the indicated multiplet members.

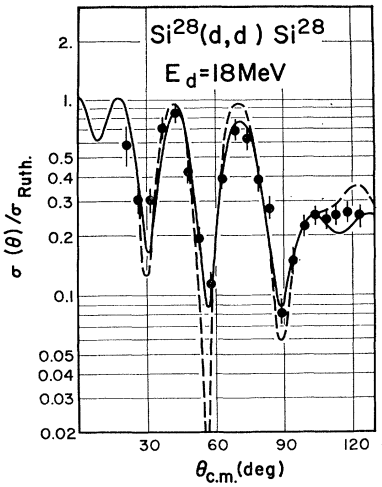

FIG. 4. 18-MeV elastic deuteron scattering optical-model fits for Si^{28}. The solid curve corresponds to line a, the dashed one to line b of the optical-model parmeter listing of Table I.

B. Optical-Model Analysis of Elastic-Scattering Angular Distributions

The angular distributions for elastic deuteron scattering at 18 MeV on Si^{28}, S^{32}, and Ar^{36} are shown in Figs. 4, 5, and 6, respectively. These data have been parametrized in terms of a standard optical model; the real part of the model potential has a Woods-Saxon form, while the imaginary part is taken as the derivative of an independent Woods-Saxon form. In particular,

$$V(r) = -\frac{V_0}{1+\exp[(r-r_0A^{1/3})/a_0]} - 4iW_i \frac{\exp[(r-r_iA^{1/3})/a_i]}{[1+\exp(r-r_iA^{1/3})/a_i]^2}.$$

We have searched automatically and simultaneously on V_0, r_0, a_0, W_i, r_i, and a_i using the search code MAGALI written by Raynal.[14] The curves superposed on the data points in Figs. 4, 5, and 6 are the best fits thus obtained, and the corresponding optical-model parameter sets are listed in Table I. As is clear from inspection, these parameters are very similar to those given earlier by Perey.[15] Indeed, as in Perey's case, we found an unusual situation and solution for the Si^{28} data where the real part of the potential is characterized by an unusually small radius and an abnormally great depth. (See Ref. b, Table II.) We believe that this may reflect our tacit assumption of a spherical model potential where we here apply it to a nonspherical nucleus. In the DWBA and coupled-channel analyses which follow, we have somewhat arbitrarily chosen to use an intermediate solution which gives much better fits to the inelastic scattering data and has parameters which are

[14] J. Raynal (private communication).
[15] C. M. Perey *et al.*, Phys. Rev. **152B**, 923 (1966).

TABLE I. Optical model parameters for an incident deuteron energy of 18.0 MeV. $r_c = 1.30$ F.

Target nucleus	V_0 (MeV)	r_0 (F)	a_0 (F)	W (MeV)	r_i (F)	a_i (F)
Si^{28}	(a) 203.467	0.6016	0.9797	24.350	1.3305	0.5997
	(b) 123.000	0.890	0.945	27.310	1.385	0.539
S^{32}	110.865	1.0053	0.8737	20.511	1.4167	0.5847
Ar^{36}	86.413	1.2148	0.513	10.90	1.6605	0.596

intuitively more reasonable (Table I, line b). The elastic scattering production of this intermediate solution is shown as the dashed curve in Fig. 4; the dominant difference in the predictions of the two solutions is clearly in the depth of the minimum near 55°. This is precisely the feature of the angular distributions which would be expected to be most sensitive to the presence of deformations, lending support to the above-mentioned assumption.

C. DWBA Analyses of Inelastic Scattering Angular Distributions

As is well known, the DWBA approach to inelastic scattering does not permit differentiation between vibrational and rotational modes. Moreover, it is strictly valid only for one-step processes, although extensions to multistep processes have been suggested. We have elected to use the DWBA approach only for the lowest 2^+ and 3^- excitations, which are expected to be strictly of a one-step character; although we have used the extensions just noted on occasion to provide corroboration of a spin assignment, we have not used them to obtain corresponding deformation parameters. Extensive discussion of these questions is available in the literature.[16,17]

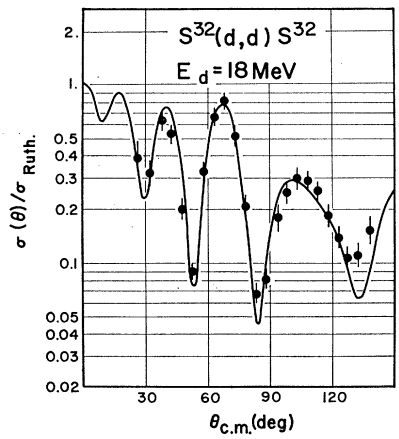

FIG. 5. 18 MeV elastic deuteron scattering optical-model fits for S^{32}. The corresponding optical-model parameters are given in Table I.

[16] G. R. Satchler, *Lectures in Theoretical Physics* (The University of Colorado Press, Boulder, Colorado 1965), p. 129.
[17] T. Tamura, Rev. Mod. Phys. **37**, 679 (1965).

The particular form of the DWBA which we have used is that of code JULIE[18]; no spin-orbit term is included in the optical-model potential used. The inelastic DWBA angular distribution is given by

$$\frac{d\sigma}{d\Omega}(\theta) = \frac{2J_f+1}{2J_i+1} \frac{|A_{lsj}|^2/(2s+1)}{5.014\times10^3} \sigma_{lsj}(\theta) \text{mb/sr},$$

where J_i and J_f are the spin of the target ground state and excited state, respectively. Here also, ℓ is the orbital angular momentum transferred to the target nucleus, **s** is the spin of the projectile, and **j** is the vector sum of ℓ and **s**.

In the case of the rotational model, the value of the matrix element A_{lsj} is given in terms of the deformation parameter β_l as

$$A_{lsj}/(2s+1) = i^l \beta_l/(2l+1),$$

and the form factor used to calculate $\sigma_{lsj}(\theta)$ in the case of a one-phonon transition is given by

$$F(r) = \frac{V_0 R_0}{a_0} \frac{d}{dx} f(x) + i \frac{W_i R_i}{a_i} \frac{d}{dx} g(x),$$

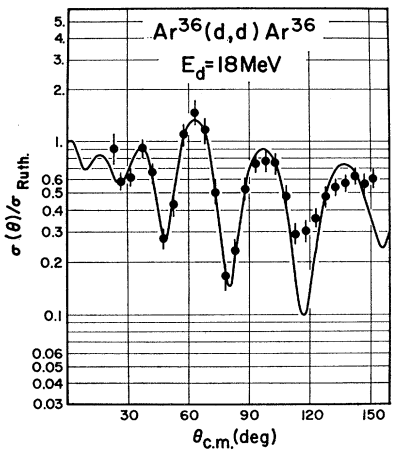

FIG. 6. 18 MeV elastic deuteron scattering optical-model fits for Ar^{36}. The corresponding optical-model parameters are given in Table I.

[18] R. H. Bassel, R. M. Drisko, and G. R. Satchler, Oak Ridge National Laboratory Report No. ORNL-3240 and Supplement, 1962 (unpublished).

where $R_0=r_0A^{1/3}$, and $R_i=r_iA^{1/3}$; $f(x)$ and $g(x)$ are, respectively, the real and imaginary form factors of the deuteron optical-model potential as defined previously.

For the spherical vibrational model, the preceding formula remain the same, except that β_l^2 is equivalent to $(2l+1)\hbar\omega_l/2C_l$, where $\hbar\omega_l$ is the centroid energy of the vibration, and C_l is the surface tension associated with the vibration.

In the case of a two-quadrupole-phonon transition, in the elementary sense of the Blair model,[19] the form factor used has no imaginary part, and we have, simply,

$$F(r)=(d^2/dx^2)f(x),$$

where $f(x)$ is the previous real form factor of the deuteron optical-model potential.

In this case,

$$A_{lsj}/(2s+1)\propto(V_0R_0^2/a_0^2)\beta_2^2, \qquad l=0, 2, 4.$$

It should be emphasized that the reaction mechanism theory on which these expressions are based is in much less satisfactory condition for the multistage processes, and the corresponding results must be treated with some caution.

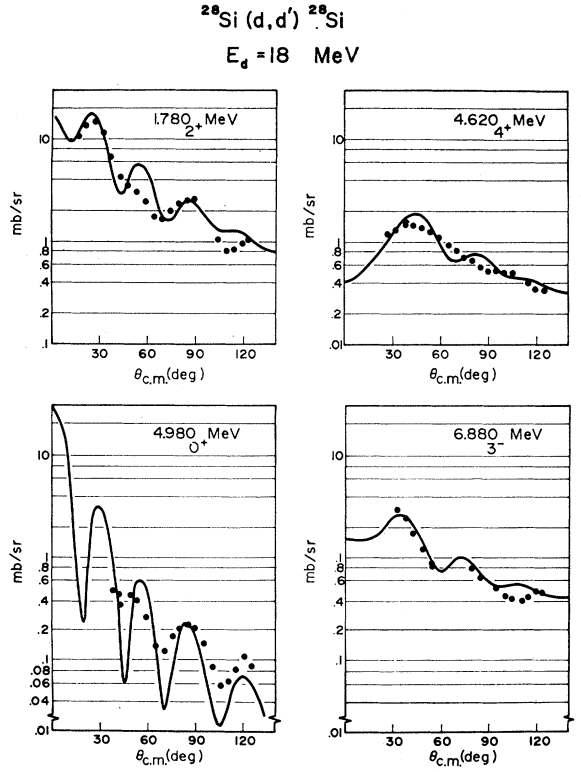

FIG. 7. Deuteron inelastic cross sections on Si^{28} at 18 MeV incident deuteron energy, together with the theoretical DWBA inelastic cross sections. The optical-model parameters used are those of Table I, and the $|\beta_l|$ values extracted from this analysis are given in Table II.

In the above expressions, we take V_0, r_0, a_0, W_i, r_i, and a_i values as fixed by the fitting to the elastic scattering angular distributions as described in the preceding section. As is then obvious, only a single parameter, the deformation β, remains free in order to normalize the model predictions to the experimental data. The errors to be assigned to the extracted $|\beta_l|$ values, it should be emphasized, are not directly proportional to those assigned to the absolute cross-section determinations, but rather to the relative errors between inelastic and elastic channels, inasmuch as the latter data are those which establish the model parameters used in extracting the β_l in a self-consistent fashion.

Figure 7 presents the angular distribution data for the four most strongly excited states in the inelastic deuteron scattering on Si^{28}, together with the corresponding DWBA fitted curves. In this case, the excitation of the 2^+, 4^+, and 3^- states at 1.78, 4.62, and 6.88 MeV is assumed to proceed via one-step processes —although this need not necessarily be the case for the 4^+ state—and the excitation of the 0^+ level at 4.98 MeV is assumed to proceed via a two-step process involving the first 2^+ state. Higher 0^+ states—in particular, that at 6.68 MeV—were not observed. Not shown here are the data for the 3^+ level at 6.28 MeV which is very weakly excited in the inelastic scattering and has an essentially isotropic angular distribution.

Figure 8 shows angular distribution data from inelastic deuteron scattering on S^{32} leading to the 2^+, 4^+, and 3^- states at 2.23-, 4.47-, and 5.01-MeV excitation. These have been selected as the candidates for DWBA analysis assuming one-phonon transitions. For comparison, the dashed and solid curves in the central figure for the 4^+ state have been calculated on the assumption of one-phonon and two-phonon processes, respectively. It is clear that the detailed structure of the predicted angular distributions is not sensitive to the details of the form factor in use. From these fits, however, it is possible to establish assignments of 4^+ and 3^- to the 4.47- and 5.01-MeV states, respectively. These assignments have recently been obtained[5] in correlation studies on deexcitation γ radiation in S^{32}, and support for them also comes from recent studies[20] of the (Li^6, d) reaction on Si^{28}.

The DWBA analysis is incapable of reproducing the angular distribution data for either the 0^+ level at 3.78 MeV or the second excited 2^+ state at 4.29 MeV. The former is essentially isotropic, and the latter shows a strong oscillatory diffraction structure. We shall return to this question in our consideration of a coupled-channel analysis below.

Figure 9 presents the angular distribution data for six states in Ar^{36} populated in the deuteron inelastic scattering at 18 MeV; also shown are four DWBA fits. Unfortunately, the energy resolution of our semiconductor detector-telescope system was not adequate to

[19] J. S. Blair, Phys. Rev. **115**, 928 (1958).

[20] N. Al Jadir, Bull. Am. Phys. Soc., **13**, 675 (1968).

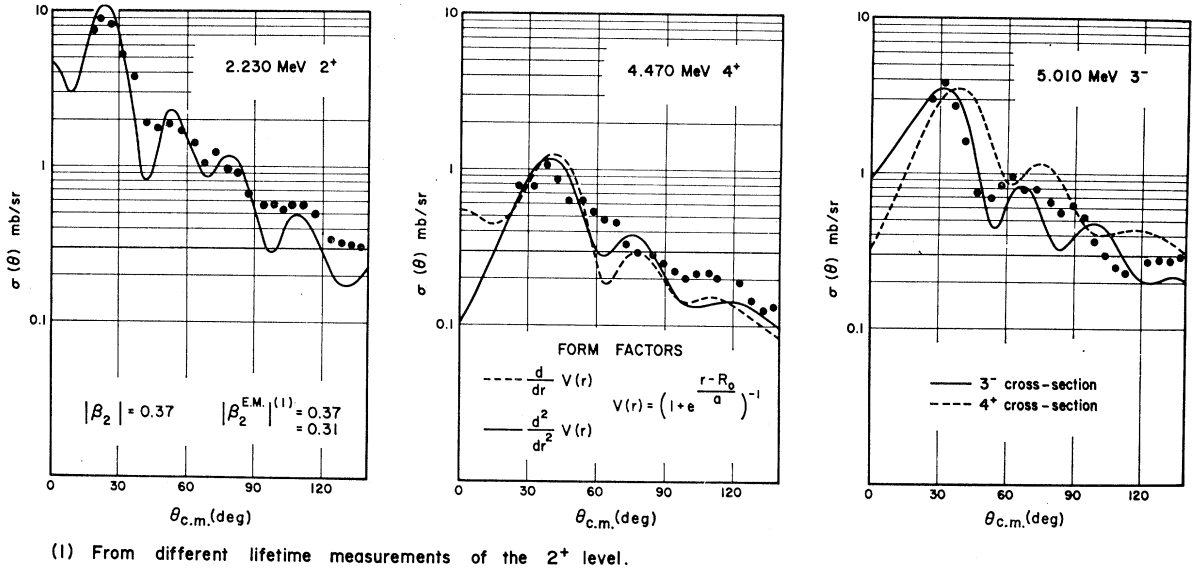

FIG. 8. Deuteron inelastic cross sections on S^{32} at 18 MeV incident deuteron energy, together with the theoretical DWBA inelastic cross sections. The optical-model parameters used are those of Table I, and the $|\beta_l|$ values extracted from this analysis are given in Table II.

permit resolution of the three closely spaced doublets of levels at 4.41, 4.98, and 5.17 MeV and of the triplet of levels at 5.89 MeV; this renders difficult any attempted analyses of the composite data. This is particularly true in the case of the 4.33-MeV doublet, where it appears that both 2^+ and 4^+ components are contributing significantly to the observed angular distribution. In the case of the other two doublets and possibly the triplet at 5.89 MeV, the observed angular distributions suggest that only one member of the doublet is involved in significant fashion. The present data establish the presence of a 3^- state at 4.98 MeV and a 5^- state at 5.17 MeV. All the curves of Fig. 9 have been calculated on the assumption of a one-step single-phonon process.

Table II summarizes the deformation-parameter data as extracted from the present measurements; as obtained from earlier DWBA analyses, where these are available; and as obtained from reduced electromagnetic transition matrix elements $B(El)$. We have the general relationship

$$B(El)\downarrow/e^2=(9/16\pi^2)[Z^2R_e^{2l}\beta_l^2/(2l+1)],$$

and we have used a standard electromagnetic radius $R_e=1.20\ A^{1/3}$. In view of the degree of arbitrariness in this selection of 1.20 F as the characteristic electromagnetic radius constant, the detailed comparison of β_l values extracted from inelastic scattering data and from electromagnetic transition strengths is of questionable significance. As indicated previously, the inelastic

TABLE II. Deformation parameters β_l.

Nucleus	Excitation energy (MeV)	J^π	$\lvert\beta_l\rvert$ from present (d,d') experiment	$\lvert\beta_l\rvert$			Electromagnetic measurement $\lvert\beta_l^{EM}\rvert$
Si^{28}	1.77	2^+	0.47	0.57[a]	0.39[b]	0.33[c]	0.40[d]
	6.88	3^-	0.33	0.46[a]	0.30[b]	0.33[c]	0.45[d]
S^{32}	2.24	2^+	0.30	0.37[a]			0.37[e]
	5.01	3^-	0.30	0.41[a]			0.33[f]
Ar^{36}	1.97	2^+	0.245		...		...
	4.178	3^-	0.31		...		...

[a] Reference 26.
[b] M. P. Frick *et al.*, in the *Proceedings of the International Conference Nuclear Physics, Gatlinburg, Tenn., 1966*, edited by R. L. Becker (Academic Press Inc., New York, 1967), p. 16.
[c] R. W. Barnard *et al.*, Nucl. Phys. **A108**, 655 (1968); (p, p') expt $E_p=21$. MeV.
[d] T. K. Alexander *et al.*, in the *Proceedings of the International Conference on Nuclear Physics, Gatlinburg, Tenn., 1966*, edited by R. L. Becker (Academic Press Inc., New York, 1967), 367
[e] P. H. Stelson *et al.*, Nucl. Data **1**, 21 (1965).
[f] R. Lombard *et al.*, Nucl. Phys. **59**, 398 (1964).

scattering, while parametrized in terms of a deformation parameter, does not in fact distinguish between rotational and vibrational modes of excitation, providing that an appropriate numerical equivalence between the β_l parameter and the characteristic phonon energy is established, i.e., $(2l+1)\hbar\omega_l/2C_l \equiv \beta_l^2$.

In the case of the 3^- state, it is probable that for all three nuclei, a coherent particle-hole configuration mixture is involved. In Ar^{36}, the second 3^- state, which was much more weakly populated than the first state in the inelastic scattering, could well have a $(1d_{3/2}^{-1}2p_{3/2})$ particle-hole configuration. Such an assumption would explain not only the rather excellent fit obtained to the experimental angular distribution data assuming a one-phonon process, but also the small $\beta_3=0.078$ value extracted from the fitting procedure. In Sec. 5 we shall adduce evidence for other components in the state as well. As is clear in Fig. 9, the fit to the data for the 5^- state at 5.18 MeV is rather poor; the value of β_5, extracted on the perhaps questionable assumption of a one-step process, is $\beta_5=0.13$.

5. COUPLED CHANNEL CALCULATIONS

In order to obtain further insight into the nature of the low-lying collective excitations in this mass region, we have applied the coupled-channel formalism developed by Tamura[21] to the inelastic scattering data presented above. In particular, we have used the code JUPITOR-1.[22] A detailed description of this code and of the coupled-channel formalism is available in the literature; however, it will be necessary to summarize the approach briefly to establish the relevant notation for our present purposes.

The coupled-channel equation set to be solved is the following:

$$\left(\frac{d^2}{d\rho_n^2}-\frac{l_n(l_n+1)}{\rho^2}-E_n^{-1}V_{\text{diag}}+1\right)R_{Jnl_nj_n}(r)=E_n^{-1}\sum_{n'l_n'j_n'}\langle(\mathcal{Y}_{l_nj_n}\otimes\Phi_{I_n})_{JM}\mid V_{\text{coupl}}\mid(\mathcal{Y}_{l_n'j_n'}\otimes\Phi_{I_n'})_{JM}\rangle R_{Jn'l_n'j_n'}(\gamma).$$

The notation is as follows: n is the ordinal number of the state in question in order of increasing excitation, i.e., $n=0$ is the ground state; $\rho_n=k_nr$ is the wave number; $\mathbf{I}_n\pi_n$ and ω_n are the spin, parity, and excitation energy of the nth target state; $E_n=E_0-\omega_n$ is the center-of-mass energy; $\mathbf{j}_n=\mathbf{l}_n+\mathbf{s}$ is the total particle angular momentum; $\mathbf{J}=\mathbf{j}_n+\mathbf{I}_n$ is the total channel angular momentum, and $R_{Jnl_nj_n}(r)$ is the radial wave function in the nth channel for a specified Jnl_nj_n quantum number set.

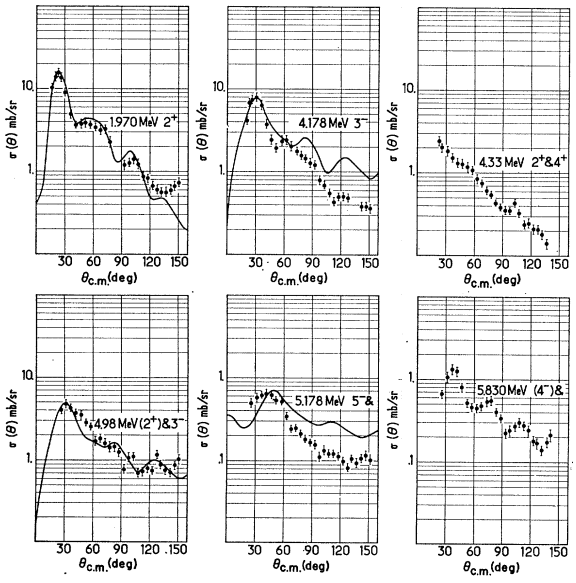

FIG. 9. Deuteron inelastic cross section on Ar^{36} at 18 MeV incident deuteron energy, together with the theoretical DWBA inelastic cross section. The optical-model parameters used are those of Table I, and the $|\beta_l|$ values extracted from this analysis are given in Table II. In the case of the deuteron groups to the higher excited multiplets, the data suggest that the dominant excitation involves the indicated multiplet member.

In the left-hand member of the coupled-channel equation set, Φ_{I_n} is the internal wave function of the target nucleus for the nth state:

$$\mathcal{Y}_{l_nj_n}(\theta,\Phi)=\sum_{m_lm_s}(lsm_lm_s\mid jm_j)i^lY_{l,m_l}(\theta,\Phi)\chi_{s,m_s},$$

where χ_{s,m_s} is the spin wave function of the scattered particle. Tamura has shown that the complex matrix elements of the right members can be expressed in the following general form:

$$\langle(\mathcal{Y}_{l_nj_n}\otimes\Phi_{I_n})_{JM}\mid V_{\text{coupl}}\mid(\mathcal{Y}_{l_n'j_n'}\otimes\Phi_{I_n'})_{JM}\rangle$$
$$\equiv\langle ljI\mid V_{\text{coupl}}\mid l'j'I'\rangle$$
$$=\sum_{t,\lambda}v_\lambda^t(r)\langle I\parallel Q_\lambda^t\parallel I'\rangle A(ljI,l'j'I',\lambda Js).$$

The function $v_\lambda^t(r)$ arises from the nondiagonal part of the general optical-model potential for a deformed nucleus, which is expanded, to second order, in powers of the product of the deformation parameter and a spherical harmonic. It follows that $v_\lambda^t(r)$ is complex. The reduced matrix element $\langle I\parallel Q_\lambda^t\parallel I'\rangle$ depends only on the internal coordinates of the target nucleus and t differentiates between terms of different character but of the same tensorial rank λ. These first two factors in the summation for the matrix elements are thus model dependent. In contrast, the multiplicative factors $A(ljI,l'j'I',\lambda Js)$, while extremely complicated, are still purely geometric and model-independent.

In the calculations we report herein, two different

[21] T. Tamura, Progr. Theoret. Phys. (Kyoto) Suppl. **37** and **38**, 683 (1966).

[22] T. Tamura, Oak Ridge National Laboratory Report No. ORNL 4152 ,1967 (unpublished).

coupling situations are relevant, depending upon whether vibrational or rotational modes of excitations are involved. We shall introduce them in sequence to define the notation and to collect the relevant reduced matrix elements $\langle I \,||\, Q_\lambda{}^t \,||\, I' \rangle$. We define the collective states $|\, I \rangle$ as follows: ground-state $|\, 0, 0 \rangle$, 0^+ level; one-quadrupole phonon state $|\, 1, 2 \rangle$, 2^+ level; one-octupole phonon state $|\, 1, 3 \rangle$, 3^- level; two-quadrupole phonon states $|\, 2, I \rangle$, $I = 0^+, 2^+, 4^+$ levels; quadrupole-octupole phonon states $|\, 2 \otimes 3, I \rangle$, $I = 1^-, 2^-, 3^-, 4^-, 5^-$ levels. We consider now the two coupling situations B I and B II as follows.

BI—Coupling for Even Spherical Vibrational Nucleus

1. Ground State, One-Quadrupole Phonon State, and Two-Quadrupole Phonon States

(a) Matrix elements having a linear dependence upon the deformation parameter:

Ground state to one-phonon state,

$$\langle 0, 0 \,||\, Q_2{}^{(1)} \,||\, 1, 2 \rangle = \beta_{02}.$$

One-quadrupole-phonon state to two-quadrupole-phonon states,

$$\langle 1, 2 \,||\, Q_2{}^{(1)} \,||\, 2, I \rangle = \beta_{2I} [2(2I+1)/5]^{1/2}; \qquad I = 0^+, 2^+, 4^+.$$

(b) Matrix elements having a quadratic dependence upon the deformation parameters:

Ground state to two-quadrupole-phonon states,

$$\langle 0, 0 \,||\, Q_\lambda{}^{(2)} \,||\, 2, I \rangle = \beta_{0I}{}^2 \delta_{I\lambda} (2200 \,|\, I0)\, (2\pi)^{-1/2}; \qquad I = 0^+, 2^+, 4^+.$$

2. Ground State, One-Quadrupole-Phonon State, One-Octupole-Phonon State, and Quadrupole-Octupole-Phonon States

(a) Matrix elements having a linear dependence upon the deformation parameters:

Ground state to one-phonon state,

$$\langle 0, 0 \,||\, Q_2{}^{(1)} \,||\, 1, 2 \rangle = \beta_{02},$$

$$\langle 0, 0 \,||\, Q_3{}^{(1)} \,||\, 1, 3 \rangle = -\beta_{03}.$$

One-quadrupole-phonon state to octupole-quadrupole-phonon state,

$$\langle 1, 2 \,||\, Q_3{}^{(1)} \,||\, 2 \otimes 3, I \rangle = \beta_{03} (-)^I [(2I+1)/7]^{1/2}; \qquad I = 1^-, 2^-, 3^-, 4^-, 5^-.$$

One octupole phonon state to one-octupole-quadrupole-phonon state,

$$\langle 1, 3 \,||\, Q_2{}^{(1)} \,||\, 2 \otimes 3, I \rangle = \beta_{02} [(2I+1)/5]^{1/2}; \qquad I = 1^-, 2^-, 3^-, 4^-, 5^-.$$

(b) Matrix elements having a quadratic dependence upon the deformation parameters:

Ground state to octupole-quadrupole-phonon state,

$$\langle 0, 0 \,||\, Q_\lambda{}^{(2)} \,||\, 2 \otimes 3, I \rangle = \beta_{02}' \beta_{03}' \delta_{\lambda I} (2300 \,|\, I0)\, (-)^{I+1} (4\pi)^{-1/2}; \qquad I = 1^-, 2^-, 3^-, 4^-, 5^-.$$

One-quadrupole-phonon state to one-octupole-phonon state,

$$\langle 1, 2 \,||\, Q_\lambda{}^{(2)} \,||\, 1, 3 \rangle = \beta_{02}' \beta_{03}' (2300 \,|\, \lambda 0)\, (4\pi)^{-1/2}.$$

In the case of a pure spherical harmonic vibrational model

$$\beta_{02} = \beta_{2I} = \beta_{0I}' = \beta_2 \quad \text{and} \quad \beta_{03} = \beta_{03}' = \beta_3,$$

however, available evidence suggests that significant deviation from such a simple model might be anticipated; in particular, the systematics of electromagnetic reduced matrix element magnitudes demonstrates that these deviations can be large.

In addition to pure two-phonon transitions, the JUPITOR-1 code permits study of predominant two-phonon situations to which, however, significant one-phonon contributions are admixed. Under such circumstances, the total matrix element connecting the ground state to the admixed state is given by

$$\langle lj0 \,|\, V_{\text{coupl}} \,|\, l'j'I \rangle = [v_I{}^{(1)}(r) \beta_{0I}'' + v_I{}^{(2)}(r) \beta_{0I}{}'^2 (2200 \,|\, I0)/(2\pi)^{1/2}] \times A(lj0, l'j'I, IJs)$$

with $I = 0^+, 2^+, 4^+$.

Of particular interest in this section is the question of sensitivity to the sign of the deformation parameter. In a pure spherical vibrational model, all the β necessarily have the same sign except for β'' which, as indicated in the above expression for the total matrix element, reflects the amplitude of the one-phonon component in the two-phonon state. The angular distribution predictions are independent of the common sign of the β_{02}, β_{2I}, and β_{0I}' parameters, but depend sensitively on the relative sign of these parameters and the β'' defined above.[21] This permits a relatively sensitive search for such one-phonon admixture amplitudes within the framework of this coupled-channel reaction model.

BII— Coupled Potential for Axially Symmetric Deformed Nucleus

Considering the ground state ($K=0$) band of an even-even nucleus, it becomes possible to obtain relatively simple expressions for the matrix elements, inasmuch as the factors $v_\lambda{}^t(r)$, now written as $v^\lambda(r)$ for simplicity, are amenable to a Legendre polynomial expansion. For a pure quadratic deformation we have

$$\langle ljI \,|\, V_{\text{coupl}} \,|\, l'j'I' \rangle = v_{\text{cp}}{}^{(2)}(r)\, (2I+1)\, (I'200 \,|\, I0)\, A(ljI, l'j'I', 2Js),$$

TABLE III. Coupling potential parameters β for the coupled-channel calculation (JUPITOR-1 code).

Reaction and coupling scheme	β_2	$\lvert\beta_2\rvert$ DWBA	I_2	β_{2I}	β_{0I}'	β_{0I}'' [a]
$Si^{28}+d$(18 MeV) Spherical vibrational model 0^+-2^+-4_2^+	0.470	0.470	0_2 2_2 4_2	0.400	0.433	−0.240[a]
$Si^{28}+d$(18 MeV) Ground-state rotational band 0^+-2^+-4^+	−0.520	0.470				
$S^{32}+d$(18 MeV) Spherical vibrational model 0^+-2_1^+-2_2^+-4_2^+	0.286	0.296	0 2_2 4_2	0.286 0.200	0.286 0.240	0.150[a] −0.180[a]

[a] Only the sign of this coefficient is determined; the other signs are either positive or negative (but not mixed). See discussion in text.

and for a pure quadratic deformation, $v_{cp}^{(2)}(r)$ is given by the following expression:

$$v_{cp}^{(2)}(r)=4\pi\int_0^1\left(\frac{-V}{1+\exp(\{r-R_0[1+\beta_2Y_{20}(\theta')]\}/a_0)}\right.$$
$$\left.-\frac{4iW_i\exp(\{r-R_i[1+\beta_2Y_{20}(\theta')]\}/a_i)}{1+\exp(\{r-R_i[1+\beta_2Y_{20}(\theta')]\}/a_i)}\right)Y_{20}(\theta')d(\cos\theta').$$

As is clear from this expression, β_2 enters linearly and thus, in principle, may have its sign determined through comparison with experimental data. Unfortunately, this β_2 dependence is not sufficiently sensitive to permit an unambiguous choice, in itself, between oblate and prolate shapes for Si^{28} as we shall see.

C. Computational Procedures

In all cases we have used the model parameters obtained through fitting the elastic scattering data; however, due recognition must be given to the fact that, since the coupled-channel formalism explicity separates out and treats the dominant inelastic channels formerly coalesced with all other inelastic processes as the source of the imaginary potential W_i, it now becomes necessary to reduce W_i below the value obtained in the elastic scattering data fits.

In addition to W_i, which we have treated as a fitting parameter, the only other free parameters are the β values which define the coupling potential. It must be emphasized that the β's and W_i are not independent.[23]

The neglect of spin orbit terms in the optical model and the restriction to even-even target nuclei results in a spinless coupled equation set and greatly reduces the requisite amount of computational time. Although the JUPITOR-1 code permits inclusion of the Coulomb potentials in calculating the coupled matrix elements, we have found in selected check situations that at 18-MeV incident deuteron energy, their inclusion results in negligible modification of the final results; we have therefore ignored these Coulomb contributions in the results to be presented below.

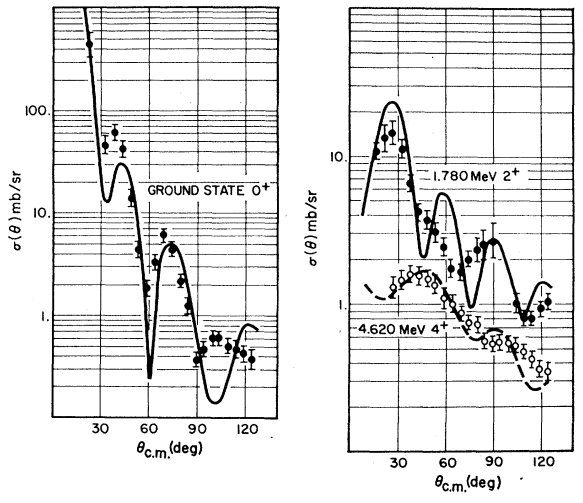

FIG. 10. Deuteron scattering cross sections for the first three levels of Si^{28}, with the theoretical cross sections given by coupled-channel caclulations on the assumption that Si^{28} is a spherical vibrational nucleus. The corresponding coupling potential parameters β are given in Table III.

D. Results of the Coupled-Channel Calculations

Figure 10 shows the results of the coupled-channel calculations[24] for the lowest 0^+, 2^+, and 4^+ states in Si^2, assuming first a spherical vibrational model. In this case, the 4^+ state is assumed to have some one-phonon admixture. The optical-model parameters used for the curves in this figure are those of Table I, line b, except that W_i has been reduced from 27.31 to 20.0 MeV; the coupling potential parameters β are given in Table III.

The fits shown in Fig. 10 are no worse than many which have been considered as definitive in the literature. However, in view of the very large value of β_{04}'' (i.e., the very large one-phonon contamination of the presumed two-phonon 4^+ configuration), coupled with the fact that the 0^+, 2^+, 4^+ excitation energies much more closely approximate a rotor spectrum than that of a vibrator, we conclude that this coupling

[23] T. Tamura, J. Phys. Soc. Japan Suppl. **24**, 288 (1968).
[24] M. C. Mermaz *et al.*, Bull. Am. Phys. Soc. **13**, 675 (1968).

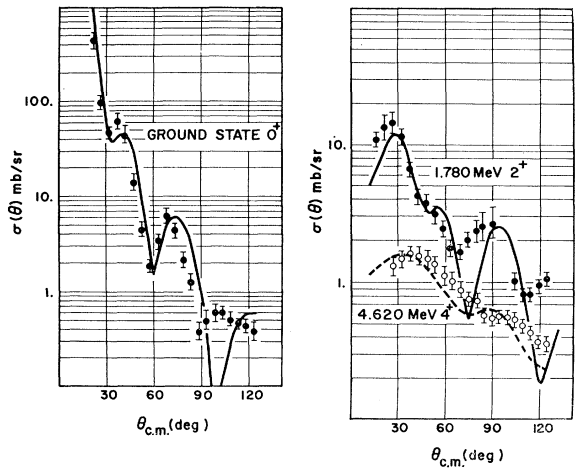

FIG. 11. Deuteron scattering cross sections for the first three levels of Si^{28} with the theoretical cross sections given by coupled-channel calculations on the assumption that Si^{28} is an axially symmetric oblate deformed nucleus, and that the 0^+, 2^+ and 4^+ states belong to the $K=0$ rotational band based on the ground state; the corresponding β_2 is given in Table III.

scheme—namely, a spherical vibrator—is of questionable applicability to Si^{28}.

With this in mind we have considered the alternative rotational coupling scheme; the results are shown in Fig. 11 for these same three states in Si.[28] The optical-model parameters remain the same, except that W_i has been reduced from 27.31 to 12.0 MeV, and the diffuseness parameter has been reduced from 0.945 to 0.745. The fact that this latter makes a very significant improvement in the fit obtained is again consistent with a static deformation for Si^{23}. When the nonsphericity of this nucleus is not explicitly incorporated into the model, as is the case in the vibrational model considered above, an anomalously large skin thickness is required to fit the experimental data. The unique $\beta_2=-0.52$ coupling potential parameter is quite consistent in magnitude with the values obtained in the corresponding DWBA analysis reported above. The rotational model provides a significantly better fit in the case of the 2^+ excitation.

Positive β_2 values give considerably poorer fits, especially in the case of the 4^+ level. However, a note of caution must be injected inasmuch as the β values and the optical-model parameters are coupled in a very complex fashion and we cannot be certain that we are using the most realistic optical potential in each given instance. Subject to this caveat, however, the evidence here available certainly supports a static oblate deformation for Si^{28}.

For S^{32}, and on the basis of the observed excitation spectrum characteristics, as discussed above, the coupled-channel calculations were based on the assumption of a spherical vibrational model. Figure 12 shows the results attained for the ground and three excited states of S^{32}, as indicated, using the optical-model parameters of Table II, except that W_i was reduced from 20.51 to 16.0 MeV. This coupling approach gains support from the fact that it couples all strongly excited positive-parity states.

The β entries in Table III indicate a relatively strong residual deviation from a simple vibrational model. Relatively large β_{0I}'' parameters are required to fit the 4^+ and 2^+_2 angular distributions.

In the case of Ar^{36}, unfortunately, the candidates for the two quadrupole phonon 2^+ and 4^+ states at 4.44 and 4.41 MeV were not experimentally resolved. Instead of considering these positive parity states as in the case of S^{32}, we here concentrate on the higher negative-parity states, namely, the second 3^- state at 4.96 MeV, the 5^- state at 5.17 MeV, and what is most probably a 4^- state at 5.89 MeV. All of these levels have unresolved neighbors, and thus the experimental angular distributions may contain significant contributions from there neighboring levels. As noted previously, the low excitation spectrum of Ar^{36} suggests a vibrational rather than a rotational approach; on this assumption, it might be suggested that the higher negative-parity states might well be the members of an octupole-quadrupole two-phonon multiplet based on the lowest

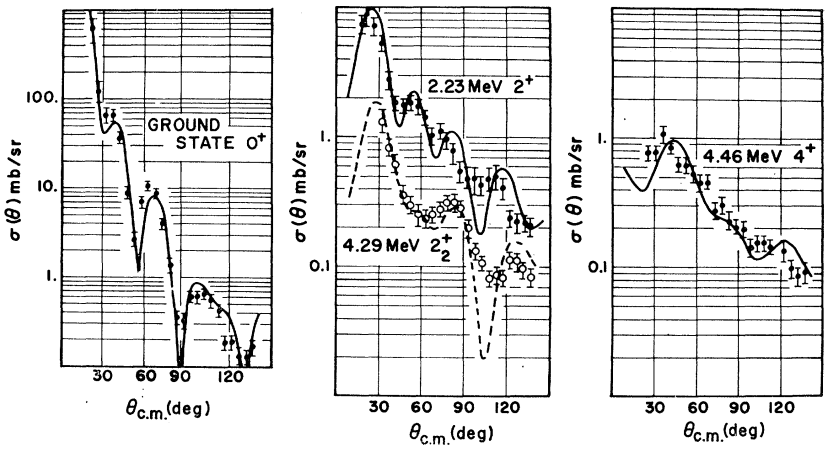

FIG. 12. Deuteron scattering cross sections for the first four strongest-excited positive-parity levels of S^{32} at 18 MeV incident deuteron energy, together with the theoretical cross sections given by coupled-channel calculations assuming that S^{32} is a spherical vibrational nucleus; the corresponding coupling potential parameters β are given in Table III.

TABLE IV. Coupling potential parameters β for the coupled-channel calculations, compared with the $|\beta_l|$ of the DWBA analysis of the $Ar^{36}+d$ system at 18-MeV incident energy.

Spherical vibrational coupling 0^+-2_1^+-3_1^+ and 3_2^- or 5_2^-		$\lvert\beta_2\rvert$	DWBA analysis $\lvert\beta_3\rvert$	$\lvert\beta_3\rvert$	$\lvert\beta_5\rvert$
		2^+	3^-	3^-	5^-
β_{02}	β_{03}	1.97 MeV	4.178 MeV	4.96 MeV	5.17 MeV
0.265	0.311	0.245	0.31	0.078	(0.130)

2^+ and 3^- states at 1.97 and 4.178 MeV, respectively. The JUPITOR-1 code permits only the simultaneous coupling of one octupole-quadrupole two-phonon state with the 0^+ ground state and with the parent 2^+ and 3^- excitations.

We have carried out three independent calculations coupling as follows: $(0^+-2_1^+-3_1^--3_2^-)$, $(0^+-2_1^+-3_1^--5_2^-)$, and $)0^+-2_1^+-3_1^--4_2^-)$, where the subscript index labels the number of phonons present. We have used the optical-model parameters of Table I except that W_i has been reduced from 10.90 to 8.90 MeV; the β values are as given in Table IV and are identical for the three calculations. The results are shown in Figure 13 for five Ar^{36} angular distributions.

The fit to the 5^- angular distribution is not impressive. It might be expected that this state should have a significant one-phonon admixture; however, the present code does not permit exploration of this possibility as was the case for 2 like-multipole phonon states. In the case of the 4^- state at 5.89 MeV, we succeeded only in reproducing the oscillatory structure in the angular distribution, while the predicted cross sections are too small by an order of magnitude.

In the case of the 4.98 MeV 3^- level, the present reasonable fit is in some sense contradictory to the DWBA analyses which assumed a one-phonon excitation mechanism. This state may well have a $(1d_{3/2}^{-1}, 2p_{3/2})$ particle-hole configuration. The corresponding $|\beta_{03}|$ is 0.078.

6. CONCLUSION

Optical-model analysis of elastic deuteron scattering at 18 MeV has established parameters for the scattering systems involving Si^{28}, S^{32}, and Ar^{36} targets.

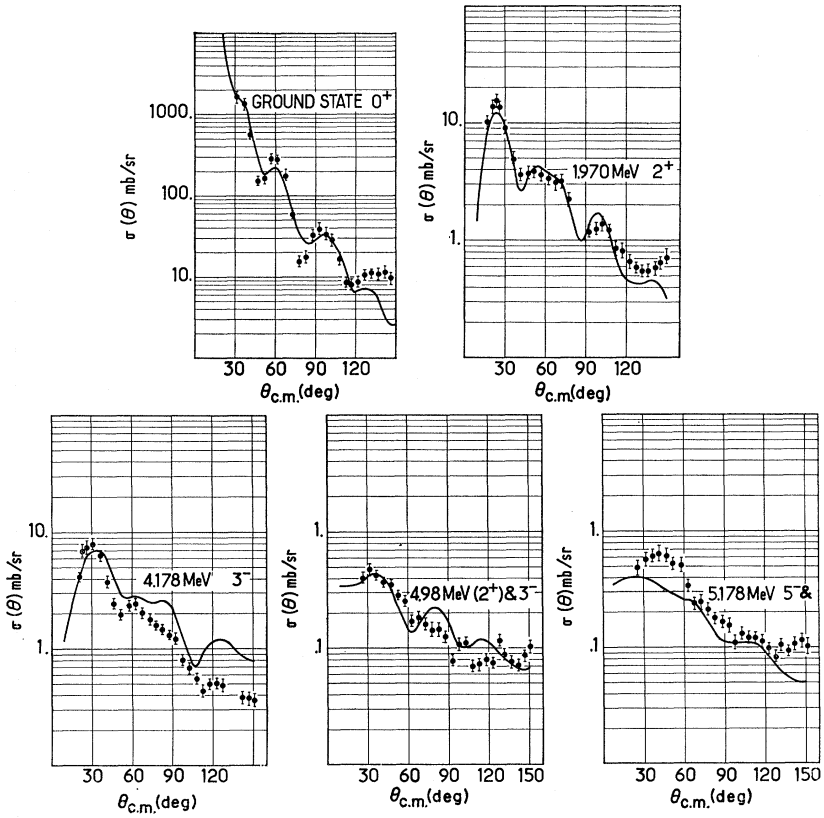

FIG. 13. Deuteron scattering cross sections for Ar^{36}, together with the theoretical cross sections given by coupled-channel calculations assuming that Ar^{36} is a spherical vibrational nucleus and that the higher negative-parity states are quadrupole-octupole-phonon states; the corresponding coupling potential parameters β are given in Table IV. It has been assumed that the dominant excitation of the multiplets at 4.96 and 5.18 MeV involve the 3^- and 5^- states, respectively.

DWBA analysis of the corresponding inelastic scattering has established $|\beta_2|$ and $|\beta_3|$ deformation parameters for the lowest lying 2^+ and 3^- excitations which are in accord with earlier results, but which do not permit differentiation between vibrational or rotational excitation modes, i.e., between static or dynamic deformations of these target nuclei.

The coupled-channel analyses have been productive in analysing the inelastic scattering data, so that it appears reasonable to conclude as follows:

Si^{28} most probably has a static oblate deformation with a $K=0$ rotational band based on the ground state. The spectroscopic factors from the $Si^{28}(dp)Si^{29}$ reaction, which we have studied and will shortly publish, provides information complementary to the inelastic scattering and also favor an oblate deformation. Recently, Alexander *et al.*[25] at Chalk River have succeeded, using the Coulomb excitation reorientation effect, in measuring the static quadrupole moment of the first excited state of both Mg^{24} and of Si^{28}. In both cases, the rotational model predicts the measured value and the signs are opposite, implying that, since Mg^{24} is prolate, therefore Si^{28} must be oblate, and that both have static deformations.

Recent attempts at fitting the inelastic proton scattering data of Crawley and Garvey[26] in the *s-d* shell utilizing a coupled-channel formalism and a rotational coupling assumption have been reported by de Swiniarski *et al.*[27] These indicate an apparent need for a significant Y_4 deformation in the Si^{28} ground state. Comparisons of the de Swiniarski *et al.* calculations with those reported herein suggest that the deuteron scattering results are much less sensitive to the presence of any such Y_4 deformation.[28]

S^{32} most probably has a spherical equilibrium shape, and its low-lying excitation spectrum comprises vibrations to this equilibrium. Spectroscopic factors obtained in our study of (d, p) and (d, t) reactions on S^{32} are extremely well-reproduced by the spherical shell-model calculations of Wildenthal *et al.*[29]

Ar^{36} also has most probably a spherical equilibrium shape. Again, remarkable agreement with the (d, p) and (d, t) spectroscopic factors is obtained in the spherical shell-model calculation of Wildenthal *et al.*[29]

As noted previously, detailed spectroscopic studies in this laboratory[6] on the $A=21$–23 systems have established that these nuclei may well be the best examples of rigid rotators in the periodic table; the present data suggest that for $32\leq A\leq 40$, at least, a spherical equilibrium shape is indicated. Recent measurements made here[30] on the $A=29$ system suggest that Al^{29} has a prolate shape, whereas Si^{29} has a relatively weak oblate shape, as is consistent with our present findings concerning Si^{28}. This over-all behavior has been reproduced grossly by the Hartree-Fock calculations of Bar-Touv and Kelson.[7] However the model reproduces neither the rapid return to sphericity beyond the midpoint of the shell, nor the weakness of the oblate deformations which seem to be indicated experimentally, nor do the model wave functions give satisfactory reproduction of the spectroscopic factors.

We shall shortly publish our detailed studies on the (d, p)[31] and (d, t)[32] reactions on Si^{28}, S^{32}, and Ar^{36}, and comparisons of the most recent model predictions with these data. As noted above, these stripping and pickup data are complementary to those presented herein.

ACKNOWLEDGMENTS

We are indebted to Kenzo Sato and the operating staff of the A. W. Wright Nuclear Structure Laboratory for their assistance during these measurements. We are much indebted to Dr. Taro Tamura for many discussions and for making available to us his JUPITOR-1 code, and to Dr. George Ripka for enlightening discussions. One of us (MCM) wishes to express his gratitude to NATO and to the Center for Nuclear Research, Saclay, for financial support.

[25] T. K. Alexander *et al.*, Bull. Am. Phys. Soc. **14**, 555 (1969).
[26] G. M. Crawley and G. T. Garvey, Phys. Rev. **160**, 891 (1967).
[27] R. de Swiniarski, C. Glashausser, D. L. Hendrie, J. Sherman, A. D. Backer, and E. A. McClatchie, Phys. Rev. Letters (to be published).
[28] C. Glashausser (private communication).
[29] B. H. Wildenthal *et al.*, Phys. Letters **29B**, 611 (1968).
[30] R. Hirko, R. Lindgren, J. Pronko, A. J. Howard, and D. A. Bromley, Bull. Am. Phys. Soc. **13**, 1371 (1968).
[31] M. C. Mermaz, C. A. Whitten, Jr., and D. A. Bromley (to be published).
[32] C. A. Whitten, Jr., M. C. Mermaz, and D. A. Bromley (to be published).